Energy & Buildings 254 (2022) 111616

Contents lists available at ScienceDirect

Energy & Buildings

journal homepage: www.elsevier.com/locate/enb

Metal-organic framework-derived graphene porous carbon matrix based lithium hydroxide chemical heat storage composite materials for residential heating

Xiangyu Yang [a,c], Shijie Li [b], Jianguo Zhao [a,b,*], Xiaomin Wang [a], Hongyu Huang [c,*], Yongzhen Wang [a]

[a] School of Materials Science and Engineering, Taiyuan University of Technology, Taiyuan 030024, PR China
[b] Institute of Carbon Materials Science, Shanxi Datong University, Datong 037009, PR China
[c] Key Laboratory of Renewable Energy, Guangdong Provincial Key Laboratory of New and Renewable Energy Research and Development, Guangzhou Institute of Energy Conversion, Chinese Academy of Sciences, Guangzhou 510640, PR China

ARTICLE INFO

Article history:
Received 5 July 2021
Revised 12 October 2021
Accepted 22 October 2021
Available online 28 October 2021

Keywords:
LiOH CHS materials
Host porous carbon matrix
Large heat storage capacity
Cycle performance
Thermal conductivity

ABSTRACT

As a promising candidate for converting renewables into chemical energy, lithium hydroxide based chemical heat storage (CHS) materials have gained great investigate enthusiasm by virtue of their outstanding storage capacity and long storage lifespan. But salt hydrates still cannot get rid of the inherent shortcomings of poor thermal conductivity, sintering, low hydration rate, and serious heat storage density degradation, Hence, it is highly desirable to create a salt hydrate CHS material that can achieve improved thermal conductivity, heat storage capacity and water storage content while maintaining good cycle stability for efficient utilization of low grade heat and residential heating. Here, we develop a lithium hydroxide composite CHS material with zeolitic imidazolate framework produced graphene-based (ZIF-8/GO) porous carbon templates as the host porous carbon matrix (ZHPCM). This Li/ZHPCM composite has huge storage strength (Max. 1483.8 kJ kg^{-1}), low reaction activation energy and high hydration capacity attribute to the adequate specific surface area and massively porous of ZHPCM, which not only boosts the spreading of lithium hydroxide, but also assuages the sintering of lithium hydroxide, thus increasing the conversion rate of LiOH to $LiOH{\cdot}H_2O$, and ultimately lead to an improvement in the storage strength. Moreover, compared to lithium hydroxide, this Li/ZHPCM composite shows remarkable cycle property for 15 times of hydration conversion without conspicuous weakened and good thermal conductivity. Besides, the calculated energy barrier that Li/ZHPCM(800)-50 (35.7 kJ mol^{-1}) needs to overcome is also significantly lower than that of lithium hydroxide (50.7 kJ mol^{-1}), which not only implies that the resistance to the reaction of Li/ZHPCM(800)-50 is smaller, but also further proves the important role of ZHPCM(800) in improving the performance of lithium hydroxide. This novel LiOH composite CHS material may paves a new way for residential heating and the further application of ZHPCM in the future.

1. Introduction

The contradiction between the substantial grow in energy caused by the rapid economic growth and the serious environmental pollution has become one of the most intractable problems facing mankind. Under such circumstances, the exploration of new renewables, energy saving as well as emission reduction technologies have become frontier hot topics in the field of energy research [1–2]. However, these renewable energies are equipped with the characteristics of timeliness and uneven output [3–4]. It is urgent to use some storage systems to preserve these precious resources and release the stored energy when needed, which overcomes the dilemma of inconsistent energy on the supply side and the demand side in time and space and improves energy utilization [5–6].

Recently, metal–organic frameworks (MOFs), a material fabricated by the coordination of metal ions and organic ligands, has captured wide interest in photocatalysis and energy storage arise from the highly adjustable crystal structure and abundant pore structure [7–8]. However, compared to carbon materials, MOFs demonstrate inferior stability to the harsh environment, which vastly narrowed its implementation scope [9]. In this context, porous carbon materials derived from MOFs have shown great

* Corresponding authors at: School of Materials Science and Engineering, Taiyuan University of Technology, Taiyuan 030024, PR China.
E-mail addresses: zhaojianguo@sxdtdx.edu.cn (J. Zhao), huanghy@ms.giec.ac.cn (H. Huang).

https://doi.org/10.1016/j.enbuild.2021.111616
0378-7788/

application potential in water adsorption as well as energy by virtue of their idiographic structure and characteristics [10–11]. Nevertheless, the collapse of the inside of the MOF crystal is inevitable during the direct pyrolysis process, so the goal of a good precursor structure required after carbonization may not be achieved [11]. In order to solve this problem, a strategy of anchoring MOFs to the carbon template (such as graphene oxide) and then carbonizing has been proposed and proved to be effective [12–13]. This type of porous carbon material integrates the characteristics of MOF with adequate specific surface area (SSA), tailorable structure, as well as the advantages of remarkable stability and heat transfer properties of carbon materials, making it a promising candidate as a host porous matrix [14–15]. Although carbon materials originated from MOFs can be found in many fields, they are rarely applied to the field of thermal energy storage, let alone chemical heat storage.

Thermal energy storage that could fill gap between energy supply and demand have attracted more and more attention around the world [16–20]. Among the common heat storage methods, the chemical heat storage has shown great commercial value in the future due to its long storage period, excellent heat storage performance and minimal energy loss [21–23]. Due to the advantages of low cost, high safety and simplicity of system operation, salt hydrates stand out among chemical heat storage (CHS) materials [24–26]. However, most of the salt hydrate CHS materials cannot be applied to low-grade heat storage owing to their high hydration requirements, resulting in a dilemma that low temperature heat cannot be fully utilized, which greatly reduces the practical application value of this type of heat storage materials [27–28]. Under such circumstances, lithium hydroxide, which has the advantages of low hydration temperature, outstanding storage strength, and non-toxicity, has turn into a research hotspot in low-grade heat storage [29–31]. Nevertheless, pristine LiOH still cannot get rid of the inherent shortcomings of poor thermal conductivity, sintering, low hydration rate, and serious heat storage density degradation of salt hydrates, which greatly limits its application potential as a low-temperature CHS material [32]. Therefore, it is still an urgent task to develop a LiOH CHS material that can achieve improved thermal conductivity, heat storage capacity and water storage content while maintaining good cycle stability for efficient utilization of low grade heat and residential heating.

In this paper, we develop a lithium hydroxide composite CHS material with zeolitic imidazolate framework/graphene-based (ZIF-8/GO) porous carbon templates as the host porous carbon matrix (ZHPCM), as shown in Scheme 1. By virtue of the adequate SSA and abundant porous, ZHPCM not only boosts the spreading of lithium hydroxide, but also assuages the sintering of lithium hydroxide. As a result, the Li/ZHPCM composite shows remarkable storage strength and high hydration rate with low reaction temperature. In addition, this Li/ZHPCM composite also exhibits exceptional cycle performance and good thermal conductivity compared to LiOH, which greatly increases its development value for residential heating and further expand the application scope of ZHPCM, as shown in Fig. 1.

2. Experimental section

2.1. Preparation of ZIF-8/GO derived host porous carbon matrix

ZIF-8/GO derived host porous carbon matrix was prepared using the modified literature procedure [33]. Typically, poly (vinylpyrrolidone) (PVP) was added to 50 mL of GO methanol solution (0.4 mg mL^{-1}) and ultrasound for 2 h to make the dispersion uniform. And $Zn(NO_3)_2$ $6H_2O$ (0.734 g) as well as 2-methylimidazole (0.851 g) were respectively dissolved in 25 mL methanol. After that, $Zn(NO_3)_2$ $6H_2O$ methanol solution was dropped to the GO/PVP mixed solution and stirred for 20 min. Then, 2-methylimidazole methanol solution was added dropwise to the previously prepared solution and reacted at 30 °C for 6 h. After the reaction was completed, the mixture was centrifuged and washed with methanol at least 4 times. After vacuum freeze drying for 48 h, the obtained ZIF-8/GO powder was heated to 800 °C at a heating rate of 5 °C min^{-1} and kept for 4 h under N_2 atmosphere. After cooling down to 30 °C at a cooling rate of 5 °C min^{-1}, the resulting black powder was immersed in HCl (2 M) for 12 h to remove the zinc component in the sample. Finally, the crude product was filtered and washed with deionized water until it was neutral, and then freeze-drying in vacuum for 8 h to obtain the target ZIF-8/GO derived host porous carbon matrix, denoted as ZHPCM(800). For comparison, ZHPCM(700) and ZHPCM(900) were synthesized through similar steps, except that the carbonization temperature was changed to 700 °C and 900 °C, respectively. Characterization is shown in Supplementary material.

3. Results and discussion

The morphologies of ZIF-8/GO, ZHPCM(800) as well as Li/ZHPCM (800)-50 are displayed in Fig. 2. Fig. 2a-b demonstrates that compared to the smooth surface of GO, the rough surface of the ZIF-8/GO proves that the ZIF-8 have successfully grown uniformly and densely on both sides of the GO surface, which forms a sandwich-like structure. This kind of sandwich-like structure can significantly reduce the sintering of ZIF/GO during carbonization [12]. After pyrolysis at high temperature, ZIF-8/GO is carbonized and converted to ZHPCM(700), ZHPCM(800) and ZHPCM(900) with partly decomposes ZIF-8 at the surface (Fig. 2c and Figure S1 and the surface of ZHPCM(700), ZHPCM(800) and ZHPCM(900) turn rougher compared to the patented ZIF-8/GO but retains the original morphology of the ZIF-8/GO. Fig. 2d demonstrates that before being composited with ZHPCM(800), the size of lithium hydroxide is bulky accompanied by serious sintering, which hinders its react with H_2O. On the contrary, Li/ZHPCM(800)-50 (Fig. 2e shows that the size of lithium hydroxide is greatly reduced and uniformly diffused on the ZHPCM(800), and the sintering phenomenon is also significantly reduced, which all contribute to the full hydration of LiOH [34].

It can be seen from the FT-IR spectra of ZIF-8, GO and ZIF-8/GO (Fig. 3a that compared to GO, the absorption peaks of ZIF-8/GO are

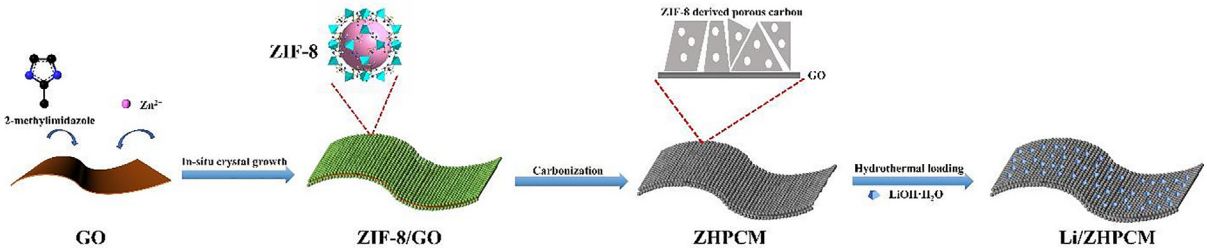

Scheme 1. Schematic demonstration of the synthesis process of Li/ZHPCM.

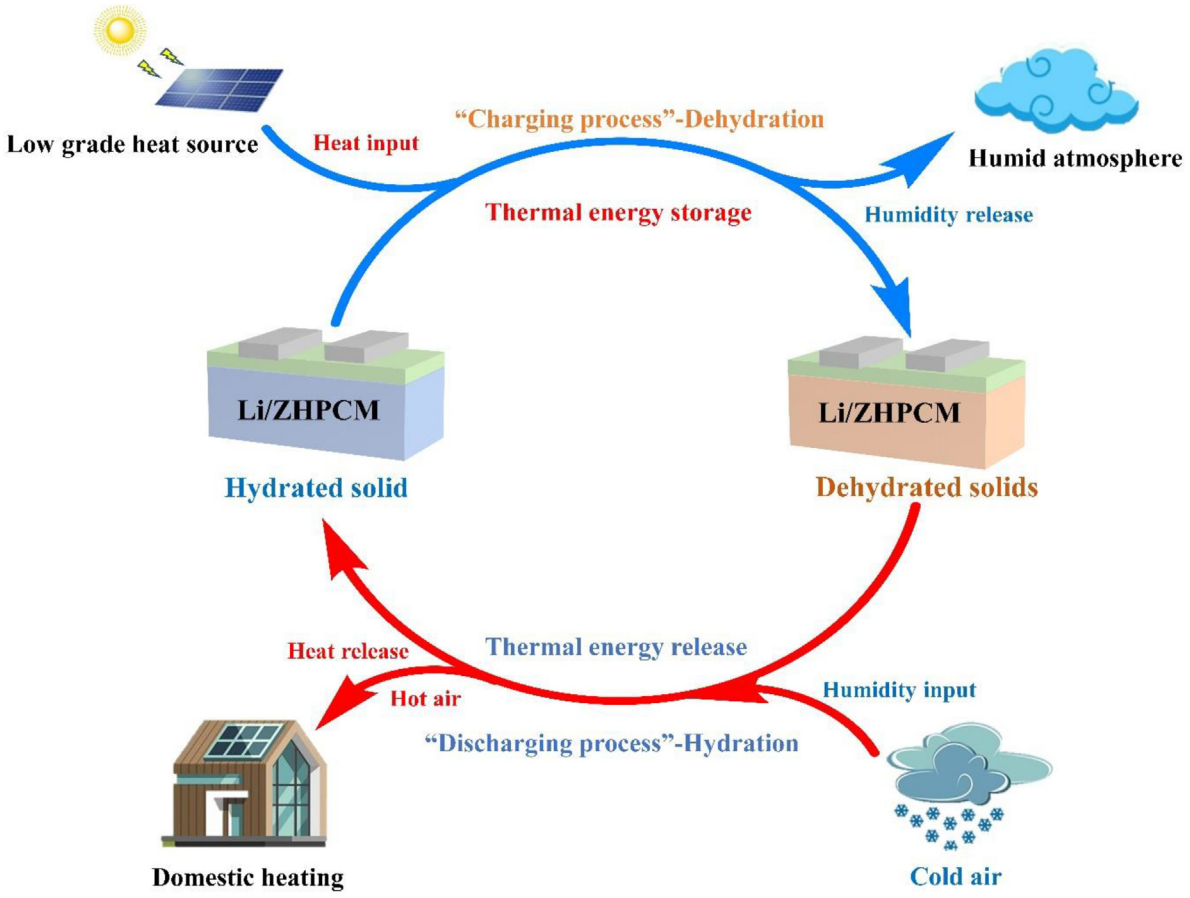

Fig. 1. Working schematic demonstration of the Li/ZHPCM for renewable energy storage and implementation.

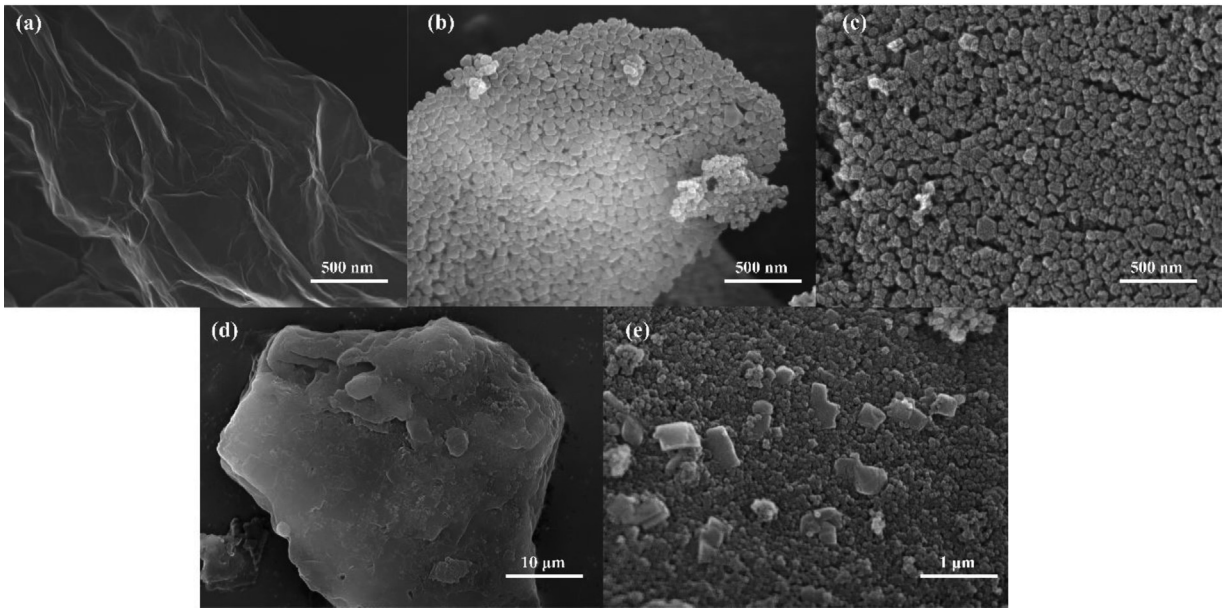

Fig. 2. SEM images of (a) GO. (b) ZIF-8/GO. (c) ZHPCM(800). (d) lithium hydroxide. (e) Li/ZHPCM(800)-50.

almost identical to those of ZIF-8, which indicates the successful uniform coating of ZIF-8 on the surface of GO. As shown in Fig. 3b, the synthesized ZIF-8 crystal shape is very good and the peaks are match with previously reported [35]. In addition, the peaks of ZIF-8/GO are basically the same as those of ZIF-8, indicating that the successful coating of ZIF-8 on the GO and the addition of graphene oxide does not change the crystal form of ZIF-8 [33]. When ZIF-8/GO undergoes carbonization, a series of characteristic peaks of ZIF-8 disappear. On the contrary, a broad peak belonging to amorphous carbon appears at about 25°, which proves that ZIF-

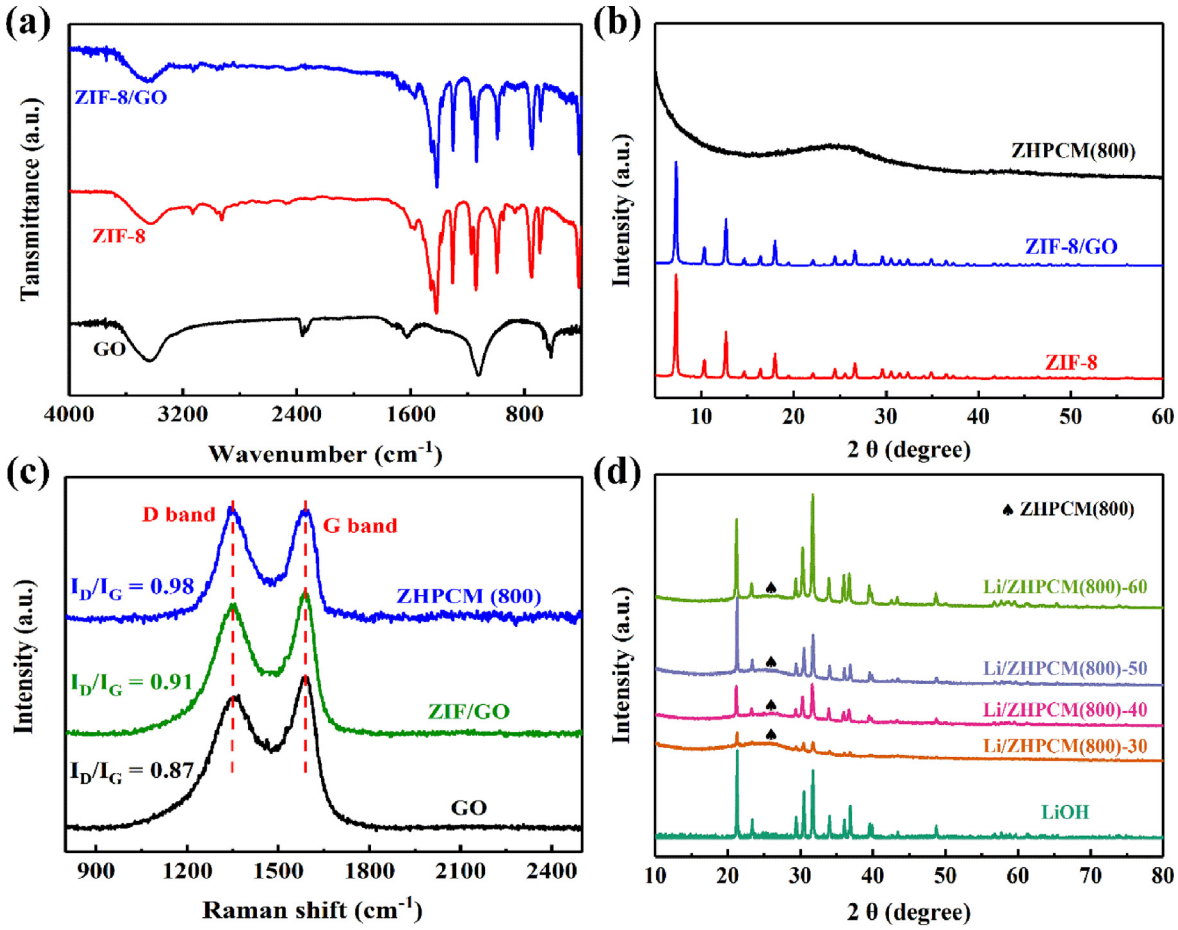

Fig. 3. (a) the FT-IR spectra of ZIF-8, GO and ZIF-8/GO. (b-c) XRD patterns and Raman spectra of ZIF-8, ZHPCM(800) and ZIF-8/GO. (d) XRD patterns of lithium hydroxide and Li/ZHPCM(800) with diverse lithium hydroxide quantity.

8/GO has been successfully converted into ZHPCM(800) with a low degree of graphitization [36]. Raman spectroscopy was performed to further analyzes the changes in graphitization and defect degree before and after carbonization. It can be seen from Fig. 3c that 1350 $cm^{-1}$and 1570 cm^{-1} respectively assign to the D band standing for amorphous carbon, and the G band representing graphitized carbon and the ratio of the two band (I_D/I_G) can indicate the degree of graphitization and defects of the material [37]. It is worth noting that compared with GO (0.87) and ZIF-8/GO (0.91), ZHPCM(800) exhibits the highest I_D/I_G value of 0.98, which shows that abundant defects and amorphous carbon are produced during the pyrolysis [38]. The increase in the degree of defects indicates that the carbonized material will have a richer porous structure, which is conducive to the good spreading of LiOH. As shown in Fig. 3d, all Li/ZHPCM(800) composites can find characteristic diffraction peaks attributed to LiOH and characteristic amorphous graphitic carbon diffraction peaks attributed to ZHPCM(800), which all indicate the successful preparation of Li/ZHPCM(800) composite materials [39].

The SSA and pore size distribution of the ZIF/GO precursor, ZHPCMs, Li/ZHPCM(800)-x were investigated through N_2 adsorption–desorption procedure. Fig. 4a demonstrates that both ZIF/GO and ZHPCM(800) display the typical Type IV isotherms, which demonstrates that the microporous and mesopores structure occupies a dominant position in the above materials [40]. Furthermore, the same conclusion that the above materials have microporous and mesopores structures can also be drawn based on the pore-size distribution curve (Fig. 4b). It is worth noting that ZHPCM (800) and Li/ZHPCM(800)-x have similar pore size distribution, which demonstrates that the load of lithium hydroxide on ZHPCM(800) does not alter the microporous and mesopore feature of ZHPCM(800). The S_{BET}, pore volume, as well as average pore size of each material are demonstrated in Table 1. It is self-evident that ZHPCM(800) shows a larger SSA (803.6 $m^2\ g^{-1}$) than that of ZHPCM (700) (456.2 $m^2\ g^{-1}$) and ZHPCM(900) (670.4 $m^2\ g^{-1}$), which means that it is an optimum candidate as host porous carbon matrix. Moreover, all Li/ZHPCM(800)-x exhibit a larger SSA than lithium hydroxide (17.4 $m^2\ g^{-1}$). Notably, compared with the traditional porous carbon material, the host matrix originated from ZIF-8/GO is equipped with a larger SSA and a richer porous, which not only facilitates the distribution of lithium hydroxide, but also mitigates the sintering of lithium hydroxide [41]. As a result, LiOH can more fully contact and react with H_2O molecules, thereby greatly improving the storage strength of the Li/ZHPCM(800) composites.

Based on the heat storage reaction mechanism of hydration-dehydration, it is self-evident that the water sorption intensity of heat storage materials under diverse environments diametrically affects the progress of the hydration reaction, which indicates that it is an major index that determines the storage strength of the CHS material. Therefore, the water sorption intensity of Li/ZHPCM(800) and lithium hydroxide under diverse RH were researched. As shown in Fig. 5a, compared to LiOH with severe sintering and larger particle size, Li/ZHPCM(800)-x composite materials have better water absorption capacity. The reason for this phenomenon is that Li/ZHPCM(800), which has adequate SSA and abundant porous, on

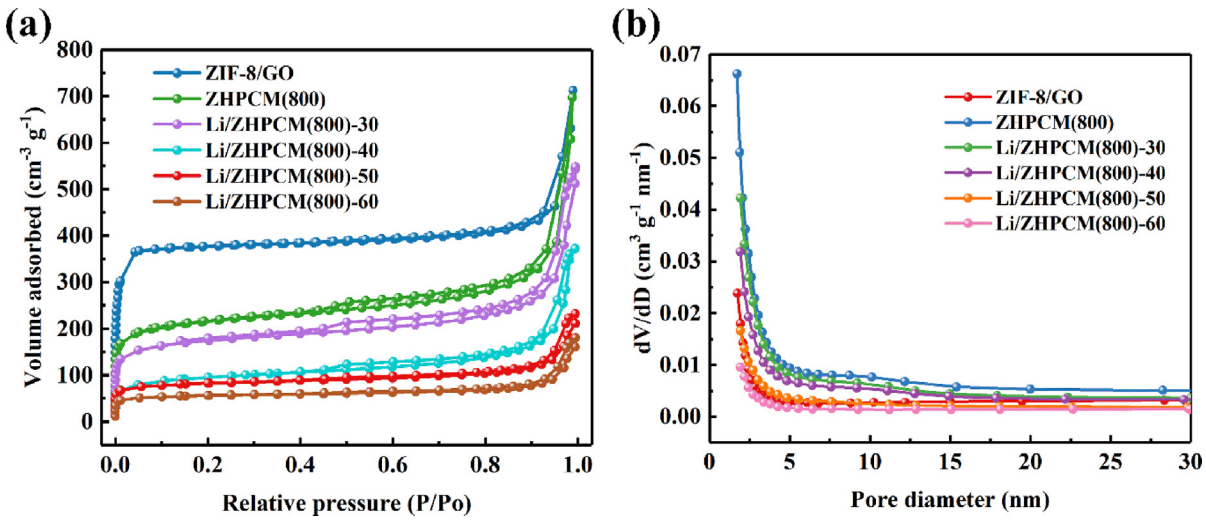

Fig. 4. (a) N_2 adsorption/desorption (b) pore size distribution of ZIF-8/GO, ZHPCM(800) and Li/ZHPCM(800) with diverse lithium hydroxide quantity.

Table 1
Pore parameters of ZIF-8/GO, ZHPCMs, Li/ZHPCM(800) as well as LiOH.

Samples	S_{BET} (m^2 g^{-1})	Total pore volume (cm^3 g^{-1})	Average pore size (nm)
ZIF-8/GO	1211.2	1.10	3.64
ZHPCM(700)	456.2	0.86	6.42
ZHPCM(800)	803.6	1.08	5.37
ZHPCM(900)	670.4	0.95	4.75
Li/ZHPCM(800)-30	557.2	0.82	8.53
Li/ZHPCM(800)-40	311.2	0.58	7.41
Li/ZHPCM(800)-50	267.0	0.36	5.34
Li/ZHPCM(800)-60	182.9	0.27	3.62
LiOH	17.4	0.08	1.78

the one hand contributes to the good spreading of lithium hydroxide, and on the other hand, it also relieves the sintering of LiOH, which reduces the hindrance of the hydration process between LiOH and H_2O molecules, thereby significantly increasing the water sorption intensity of Li/ZHPCM(800) [34]. Furthermore, the water sorption intensity of the Li/ZHPCM(800) under each RH is matched with the lithium hydroxide quantity change trend between 30% and 50%, and when the lithium hydroxide quantity is the same, the water sorption intensity of Li/ZHPCM(800) also increases with the increase of RH, which shows that the water sorption intensity of Li/ZHPCM(800)-x depends on both the lithium hydroxide quantity and RH. On the contrary, when the lithium hydroxide quantity is increased from 50% to 60%, the water sorption intensity of the Li/ZHPCM(800) decreases at each RH. And the detailed water absorption capacity of each sample at various RH are demonstrated in Table S1. This could be stemmed from the excessively high lithium hydroxide quantity in Li/ZHPCM(800)-60 aggravating the sintering of LiOH on its surface, which hinders the good spreading of LiOH on the surface of ZHPCM(800) and causes LiOH particle size to become larger, which eventually leads to a decrease in its water absorption capacity [42]. The SEM (Fig. 5b results also confirmed this conclusion. Therefore, Li/ZHPCM(800)-50 with the best water absorption capacity among all tested samples is ideal for seasonal heat storage in residential heating.

To find out the influence of different pyrolysis temperatures on the storage strength of composite materials, STA was performed to investigate the storage strength of samples under various pyrolysis conditions. As shown in Fig. 6 and Fig. 7d, Li/ZHPCM(800)-50 (1483.8 kJ kg^{-1}) exhibits the highest storage strength compared to Li/ZHPCM(700)-50 (554.1 kJ kg^{-1}) as well as Li/ZHPCM(900)-50 (927.8 kJ kg^{-1}). The reason for this phenomenon is that compared with the other two, ZHPCM(800) shows a larger SSA and porous according to the BET result, which contributes to the better diffusion of LiOH on its surface and the interact with H_2O mole-

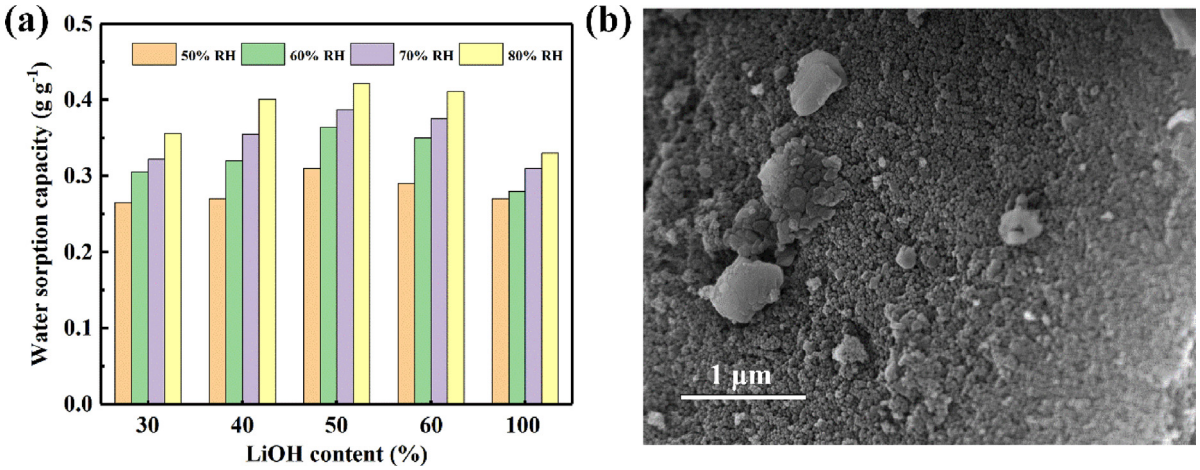

Fig. 5. (a) water adsorption capacity of Li/ZHPCM(800) with diverse lithium hydroxide quantity and lithium hydroxide with various RH. (b) SEM image of Li/ZHPCM(800)-60.

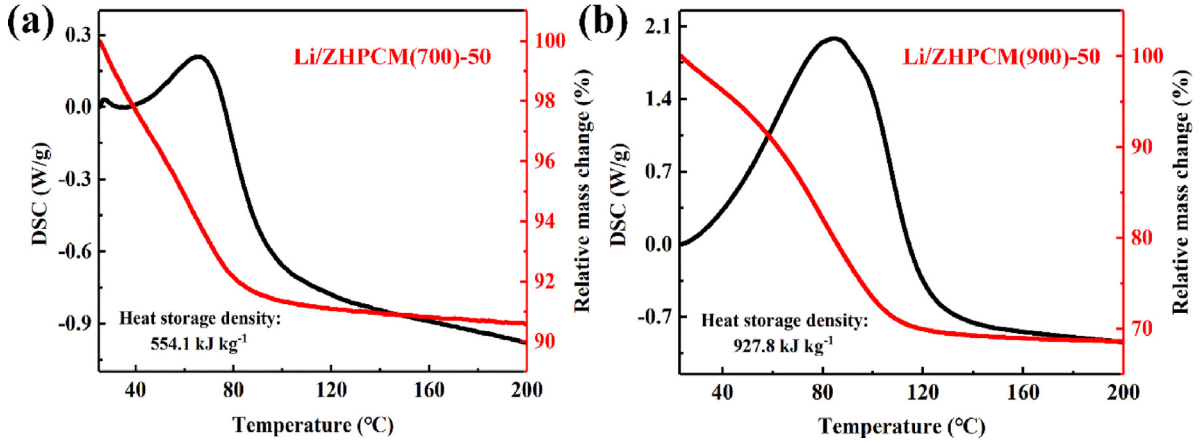

Fig. 6. STA curves of (a) Li/ZHPCM(700)-50, (b) Li/ZHPCM(900)-50.

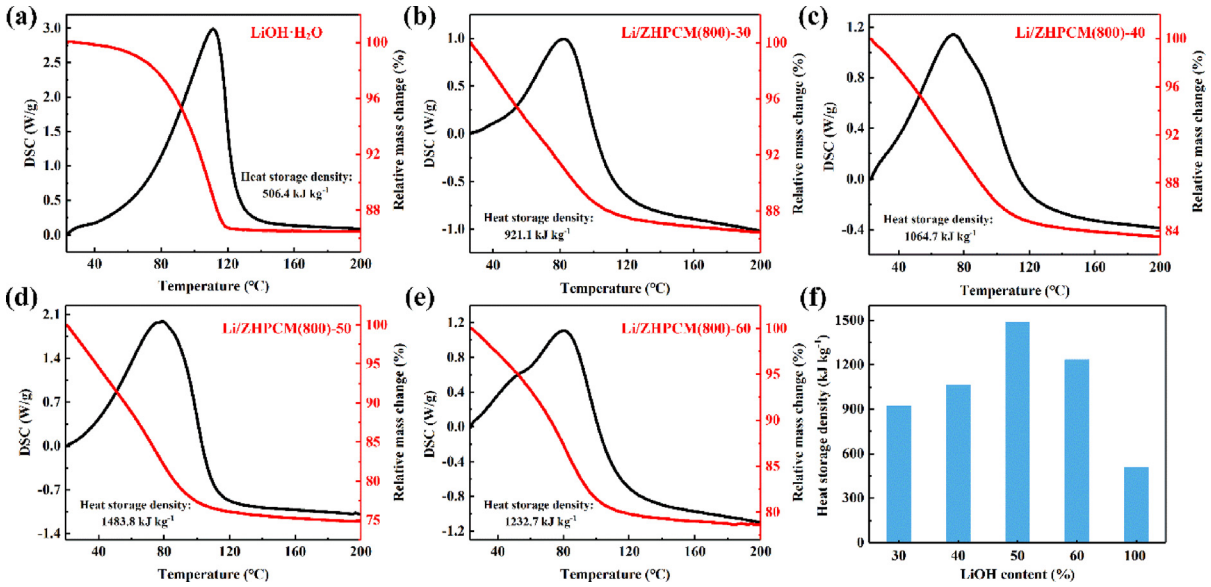

Fig. 7. STA curves of (a) LiOH·H_2O and (b-e) Li/ZHPCM(800) with diverse lithium hydroxide quantity. (f) the variation trend of storage strength with lithium hydroxide quantity of Li/ZHPCM(800).

cules, and thus makes Li/ZHPCM(800)-50 exhibit better heat storage performance.

The storage strength of lithium hydroxide and Li/ZHPCM(800) were also investigated. As shown in Fig. 7a, the storage strength of the lithium hydroxide can just reach 506.4 kJ kg^{-1}, which is caused by the inability to fully hydrate the LiOH with H_2O molecules due to the bulky size and sintering of the lithium hydroxide. This result indicates that the low conversion rate between LiOH and LiOH·H_2O is an important reason hindering the improvement of the performance of LiOH heat storage materials. In Fig. 7b-e, it is self-evident that after LiOH is composited with ZHPCM(800), the storage strength of each Li/ZHPCM(800)-x has shown a significant increase compared with lithium hydroxide, and the storage strength of Li/ZHPCM(800)-50 can reach up to 1483.8 kJ kg^{-1}, which is 293% stronger than that of lithium hydroxide. The reason for this phenomenon is that Li/ZHPCM(800) with an adequate SSA and abundant porous not only has a positive effect on the spreading of lithium hydroxide, but also reduces the sintering of lithium hydroxide particles, which increase the conversion rate of LiOH to LiOH·H_2O, thus leading to an improvement in the storage strength of Li/ZHPCM(800) [34]. Notably, when the lithium hydroxide quantity is increased from 30% to 50%, the storage strength of Li/ZHPCM (800) composites is also improved accordingly, but when it raises to 60%, the storage strength of Li/ZHPCM(800)-60 is lower than that of Li/ZHPCM(800)-50 (Fig. 7f. This is arising from the excessive amount of LiOH in Li/ZHPCM(800)-60, which aggravates the sintering of LiOH on its surface, and thus causes the bulking of lithium hydroxide and the inability to uniformly disperse on the surface of Li/ZHPCM(800)-60. As a result, the hydration reaction rate is reduced and eventually leads to a decrease in storage strength of the composites [41]. It is worth noting that this result corresponds to the water sorption intensity result, which confirms the inseparable connection between the hydration conversion rate and the storage strength. From the above results, it can be concluded that Li/ZHPCM(800)-50, which has remarkable storage strength and outstanding hydration conversion rate, has demonstrated huge development capital in high efficiency and seasonal heat storage of low grade heat for residential heating.

Like storage strength, cycle stability also has a crucial impact on the practical application of chemical heat storage materials. Therefore, an alternative hydration ↔ dehydration process was performed to investigate the cycle ability of Li/ZHPCM(800)-50,

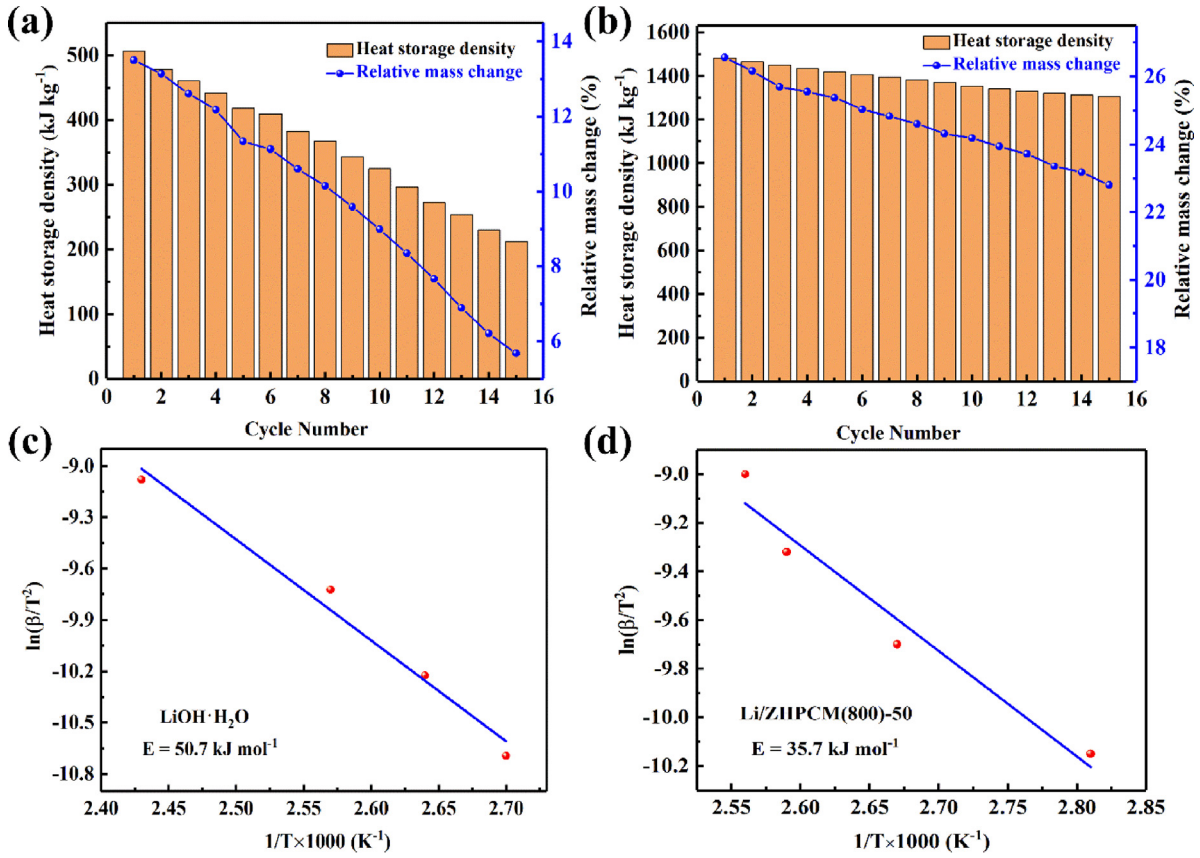

Fig. 8. Trends of related heat storage parameters and the activation energy of (a, c) lithium hydroxide (b, d) Li/ZHPCM(800)-50.

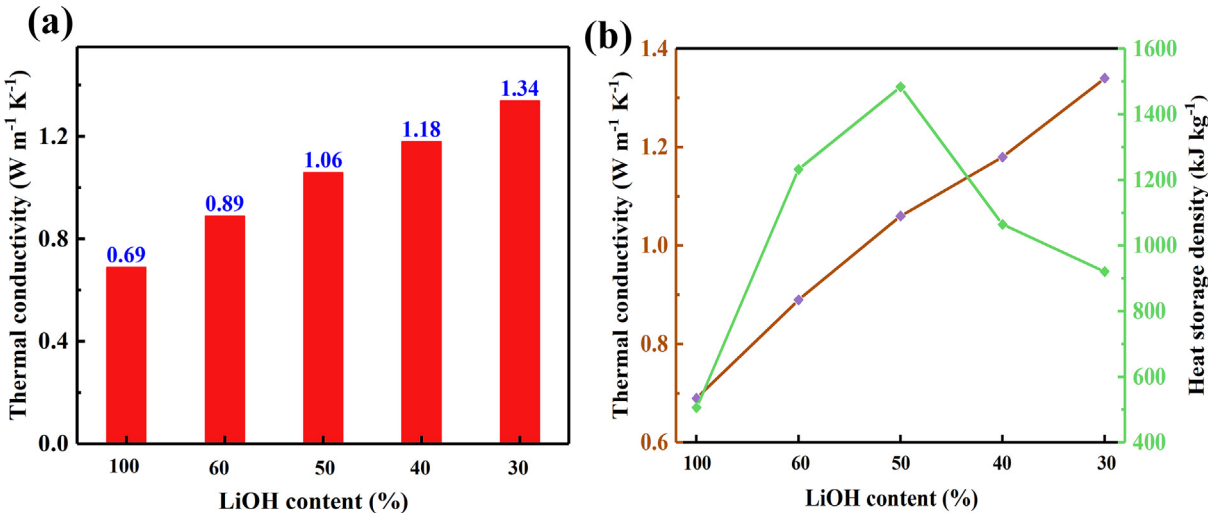

Fig. 9. (a) Thermal conductivity (b) The relationship between heat transfer property and heat storage strength of lithium hydroxide and Li/ZHPCM(800) with diverse lithium hydroxide quantity.

which has the best storage strength. Each cycle has performed the same steps as STA, and the normalized relative mass change (RMC) is stood for the water sorption intensity, so that the water sorption intensity changes during the entire cycle can be observed. As shown in Fig. 8a-b, the storage strength and RMC of both Li/ZHPCM(800)-50 and LiOH decrease with increase of the cycle process, but there is a clear difference in the degree of decrease between the two samples. After 15 cycles, the storage strength of lithium hydroxide (Fig. 8a decreased from 506.4 to 212.4 kJ kg^{-1} by 58.1%; and the RMC dropped from 13.5% to 5.6% by 58.5%, which is a relatively sharp drop. While the storage strength of Li/ZHPCM (800)-50 (Fig. 8b dropped from 1483.8 to 1307.2 kJ kg^{-1} by 11.9%; and the RMC dropped from 26.6% to 22.8% by 14.2%, which is a relatively gentle downward trend after 15 cycles. The reason for this

Table 2
Key storage strength indicators of diverse CHS composites

Salt hydrate	Dehydration temperature (°C)	Host matrix	Water sorption intensity (g g^{-1})	Storage ability (kJ kg^{-1})	Thermal conductivity (W $m^{-1}·K^{-1}$)	Activation Energy (kJ mol^{-1})	Ref.
$SrBr_2$	250	Expanded graphite	0.34	850	5.57	\	[43]
$CaCl_2$	200	Silica-alumina	0.4	700	\	\	[24]
$Ca(OH)_2$	310	$ZrO(NO_3)_2$	0.25	1125	\	138.1	[25]
LiCl	90	silica gel	\	450	\	\	[44]
$MgSO_4$	120	$ZnSO_4$	0.23	1422	\	\	[26]
$Mg(OH)_2$	350	GO	\	765	1.23	38.2	[27]
LiOH	80	ZHPCM (800)	0.42	1483.8	1.06	35.7	This work

phenomenon is that the degree of sintering of LiOH particles in Li/ZHPCM(800)-50 is less serious than that of LiOH during the cycle, and the energy barrier that Li/ZHPCM(800)-50 (35.7 kJ mol^{-1}) needs to overcome is also greatly lower than that of lithium hydroxide (50.7 kJ mol^{-1}) according to Fig. 8c-d, which both allows Li/ZHPCM(800)-50 to hydrate relatively well with H_2O molecules, resulting in a lighter degree of degradation of Li/ZHPCM(800)-50 after the cycle [31].

In addition, thermal conductivity is also a vital indicator to assess the practical application value of chemical heat storage materials. In Fig. 9a, it is self-evident that due to the remarkable heat transfer properties of the host matrix, all Li/ZHPCM(800)-x composites exhibit better thermal conductivity than lithium hydroxide, and the heat transfer performance of Li/ZHPCM(800)-30 (1.34 W $m^{-1}·K^{-1}$) is 194% stronger than that of lithium hydroxide (0.69 W $m^{-1}·K^{-1}$). As shown in Fig. 9b, it is also worth noting that although the heat transfer property and storage strength of Li/ZHPCM(800) show a diametrically opposite trend with the content of LiOH, it is further determined that Li/ZHPCM(800)-50 is the most optimum LiOH composite CHS material in this work after comprehensive consideration of the actual heat transfer and storage capacity. Notably, by comparing some key storage strength indicators of various heat storage materials in Table 2, it can be found that the storage strength of Li/ZHPCM(800)-50 has also shown a significant improvement under the premise of a lower charging temperature [24–27,43,44].

4. Conclusion

In summary, we have successfully proved that Li/ZHPCM(800) is an excellent LiOH composite CHS material with outstanding storage performance and cycle stability. The structure properties of ZHPCM(800) and Li/ZHPCM(800) have been fully characterized and demonstrated. Water sorption intensity of lithium hydroxide and Li/ZHPCM(800) in different environments is investigated to assess the hydration capability. Investigation of important parameters (heat storage density, cycling stability) that closely related to heat storage performance is conducted. The decisive parameter of heat transfer performance, thermal conductivity, and the index of the difficulty of reaction progress, activation energy have also been studied. The results are as follows:

a) XDR and Reman results demonstrates that the successful conversion of ZIF-8/GO to ZHPCM (800) with high degree of defects and the combination of lithium hydroxide with ZHPCM (800).
b) SEM and BET results shows that ZHPCM(800) not only retains the feature morphology of the ZIF-8/GO, but also has the merits adequate SSA (803.6 m^2 g^{-1}) and pore volume (1.08 cm^3 g^{-1}), which makes it a promising candidate as a host porous matrix.
c) By virtue of the large SSA and good porosity, ZHPCM(800) not only boosts the spreading of lithium hydroxide, but also assuages the sintering of lithium hydroxide, which leads to the improvement of the storage strength up to 1483.8 kJ kg^{-1} and water adsorption ability of Li/ZHPCM(800) composites.
d) Li/ZHPCM(800)-50 composite also shows exceptional cycle property for 15 times of hydration conversion without conspicuous weakened and outstanding thermal conductivity (1.06 W $m^{-1}·K^{-1}$).
e) The calculated activation energy of Li/ZHPCM(800)-50 (35.7 kJ mol^{-1}) is much lower than that of lithium hydroxide (50.7 kJ mol^{-1}), which further promotes its excellent storage performance.

It can be demonstrated that Li/ZHPCM(800) with outstanding storage performance as well as excellent cyclic stability and thermal conductivity provides a new approach for converting renewables into chemical energy and seasonal heat storage in residential heating and may also sheds light on new avenues for residential heating and the upcoming widespread application of ZHPCM.

Declaration of Competing Interest

The authors declare that they have no known competing financial interests or personal relationships that could have appeared to influence the work reported in this paper.

Acknowledgements

The authors appreciate the support from Research and development projects in key areas of Guangdong Province (Grant No. 2020B0202010004). National Natural Science Foundation of China (Grant No. 52071192), Key Research Program of Frontier Sciences, CAS, (Grant No. QYZDY-SSW-JSC038).

Appendix A. Supplementary data

Supplementary data to this article can be found online at https://doi.org/10.1016/j.enbuild.2021.111616.

References

[1] N. Armaroli, V. Balzani, The future of energy supply: challenges and opportunities, Angew. Chem. Int. Ed. 46 (1-2) (2007) 52–66.
[2] A.J. Carrillo, J. González-Aguilar, M. Romero, J.M. Coronado, Solar energy on demand: a review on high temperature thermochemical heat storage systems and materials, Chem. Rev. 119 (7) (2019) 4777–4816.
[3] A. Gil, M. Medrano, I. Martorell, A. Lázaro, P. Dolado, B. Zalba, L.F. Cabeza, State of the art on high temperature thermal energy storage for power generation. Part 1—concepts, materials and modellization, Renew. Sustain. Energy Rev. 14 (1) (2010) 31–55.

[4] F. Marias, P. Neveu, G. Tanguy, P. Papillon, Thermodynamic analysis and experimental study of solid/gas reactor operating in open mode, Energy 66 (2014) 757–765.
[5] T. Yan, T. Li, J. Xu, J. Chao, R. Wang, Y.I. Aristov, L.G. Gordeeva, P. Dutta, S.S. Murthy, Ultrahigh-energy-density sorption thermal battery enabled by graphene aerogel-based composite sorbents for thermal energy harvesting from air, ACS Energy Lett. 6 (5) (2021) 1795–1802.
[6] R.-J. Clark, A. Mehrabadi, M. Farid, State of the art on salt hydrate thermochemical energy storage systems for use in building applications, J. Storage Mater. 27 (2020) 101145.
[7] L. Yang, X. Zeng, W. Wang, D. Cao, Recent progress in MOF-derived, heteroatom-doped porous carbons as highly efficient electrocatalysts for oxygen reduction reaction in fuel cells, Adv. Funct. Mater. 28 (7) (2018) 1704537.
[8] J. Song, C. Zhu, B.Z. Xu, S. Fu, M.H. Engelhard, R. Ye, D. Du, S.P. Beckman, Y. Lin, Bimetallic Cobalt-based phosphide zeolitic imidazolate framework: CoPx phase-dependent electrical conductivity and hydrogen atom adsorption energy for efficient overall water splitting, Adv. Energy Mater. 7 (2) (2017) 1601555.
[9] L.G. Gordeeva, Y.D. Tu, Q. Pan, M.L. Palash, B.B. Saha, Y.I. Aristov, R.Z. Wang, Metal-organic frameworks for energy conversion and water harvesting: a bridge between thermal engineering and material science, Nano Energy 84 (2021) 105946.
[10] W. Shi, Y. Zhu, C. Shen, J. Shi, G. Xu, X. Xiao, R. Cao, Water sorption properties of functionalized MIL-101(Cr)-X (X=-NH2, –SO3H, H, –CH3, –F) based composites as thermochemical heat storage materials, Microporous Mesoporous Mater. 285 (2019) 129–136.
[11] K. Wang, K.N. Hui, K. San Hui, S. Peng, Y. Xu, Recent progress in metal–organic framework/graphene-derived materials for energy storage and conversion: design, preparation, and application, Chemical Science, 12 (16) (2021) 5737-5766.
[12] J. Wei, Y. Hu, Y. Liang, B. Kong, J. Zhang, J. Song, Q. Bao, G.P. Simon, S.P. Jiang, H. Wang, Nitrogen-doped nanoporous carbon/graphene nano-sandwiches: synthesis and application for efficient oxygen reduction, Adv. Funct. Mater. 25 (36) (2015) 5768–5777.
[13] Wenhao Liu, Kai Wang, Chen Li, Xiong Zhang, Xianzhong Sun, Jianwei Han, Xing-Long Wu, Feng Li, Yanwei Ma, Boosting solid-state flexible supercapacitors by employing tailored hierarchical carbon electrodes and a high-voltage organic gel electrolyte, J. Mater. Chem. A 6 (48) (2018) 24979–24987.
[14] Anastasia Permyakova, Sujing Wang, Emilie Courbon, Farid Nouar, Nicolas Heymans, Pierre D'Ans, Nicolas Barrier, Pierre Billemont, Guy De Weireld, Nathalie Steunou, Marc Frère, Christian Serre, Design of salt–metal organic framework composites for seasonal heat storage applications, J. Mater. Chem. A 5 (25) (2017) 12889–12898.
[15] Luis Garzón-Tovar, Javier Pérez-Carvajal, Inhar Imaz, Daniel Maspoch, Composite salt in porous metal-organic frameworks for adsorption heat transformation, Adv. Funct. Mater. 27 (21) (2017) 1606424.
[16] P. Fleuchaus, B. Godschalk, I. Stober, P. Blum, Worldwide application of aquifer thermal energy storage – a review, Renew. Sustain. Energy Rev. 94 (2018) 861–876.
[17] Y. Zhang, R. Wang, Sorption thermal energy storage: concept, process, applications and perspectives, Energy Storage Mater. 27 (2020) 352–369.
[18] Mehmet Esen, Teoman Ayhan, Development of a model compatible with solar assisted cylindrical energy storage tank and variation of stored energy with time for different phase change materials, Energy Convers. Manage. 37 (12) (1996) 1775–1785.
[19] Mehmet Esen, Aydin Durmuş, Ayla Durmuş, Geometric design of solar-aided latent heat store depending on various parameters and phase change materials, Sol. Energy 62 (1) (1998) 19–28.
[20] Mehmet Esen, Thermal performance of a solar-aided latent heat store used for space heating by heat pump, Sol. Energy 69 (1) (2000) 15–25.
[21] S. Bennici, T. Polimann, M. Ondarts, E. Gonze, C. Vaulot, N. Le Pierrès, Long-term impact of air pollutants on thermochemical heat storage materials, Renew. Sustain. Energy Rev. 117 (2020) 109473.
[22] P.A.J. Donkers, L.C. Sögütoglu, H.P. Huinink, H.R. Fischer, O.C.G. Adan, A review of salt hydrates for seasonal heat storage in domestic applications, Appl. Energy 199 (2017) 45–68.
[23] G. Alva, Y. Lin, G. Fang, An overview of thermal energy storage systems, Energy 144 (2018) 341–378.
[24] A. Jabbari-Hichri, S. Bennici, A. Auroux, Enhancing the heat storage density of silica–alumina by addition of hygroscopic salts (CaCl2, Ba(OH)2, and LiNO3), Sol. Energy Mater. Sol. Cells 140 (2015) 351–360.
[25] Y.-T. Li, M.-T. Li, Z.-B. Xu, Z.-H. Meng, Q.-P. Wu, Dehydration kinetics and thermodynamics of ZrO(NO3)2-doped Ca(OH)2 for chemical heat storage, Chem. Eng. J. 399 (2020) 125841.
[26] A.U. Rehman, M. Khan, Z. Maosheng, Hydration behavior of MgSO4–ZnSO4 composites for long-term thermochemical heat storage application, J. Storage Mater. 26 (2019) 101026.
[27] Shijie Li, Hongyu Huang, Xixian Yang, Chenguang Wang, Noriyuki Kobayashi, Mitsuhiro Kubota, A facile method to construct graphene oxide-based magnesium hydroxide for chemical heat storage, Nanoscale Microscale Thermophys. Eng. 21 (1) (2017) 1–7.
[28] Luigi Calabrese, Vincenza Brancato, Valeria Palomba, Andrea Frazzica, Luisa F. Cabeza, Magnesium sulphate-silicone foam composites for thermochemical energy storage: assessment of dehydration behaviour and mechanical stability, Sol. Energy Mater. Sol. Cells 200 (2019) 109992.
[29] M. Kubota, S. Matsumoto, H. Matsuda, H.Y. Huang, Z.H. He, X.X. Yang, Chemical heat storage with LiOH/LiOH·H2O reaction for low-temperature heat below 373 K, Adv. Mater. Res. 953–954 (2014) 757–760.
[30] M. Kubota, S. Matsumoto, H. Matsuda, Enhancement of hydration rate of LiOH by combining with mesoporous carbon for low-temperature chemical heat storage, Appl. Therm. Eng. 150 (2019) 858–863.
[31] W. Li, J.J. Klemeš, Q. Wang, M. Zeng, Development and characteristics analysis of salt-hydrate based composite sorbent for low-grade thermochemical energy storage, Renewable Energy 157 (2020) 920–940.
[32] W. Li, J.J. Klemeš, Q. Wang, M. Zeng, Energy storage of low potential heat using lithium hydroxide based sorbent for domestic heat supply, J. Cleaner Prod. 285 (2021) 124907.
[33] Hai-xia Zhong, Jun Wang, Yu-wei Zhang, Wei-lin Xu, Wei Xing, Dan Xu, Yue-fei Zhang, Xin-bo Zhang, ZIF-8 derived graphene-based nitrogen-doped porous carbon sheets as highly efficient and durable oxygen reduction electrocatalysts, Angew. Chem. Int. Ed. 53 (51) (2014) 14235–14239.
[34] S. Li, H. Huang, X. Yang, Y. Bai, J. Li, N. Kobayashi, M. Kubota, Hydrophilic substance assisted low temperature LiOH·H2O based composite thermochemical materials for thermal energy storage, Appl. Therm. Eng. 128 (2018) 706–711.
[35] F. Zheng, Y. Yang, Q. Chen, High lithium anodic performance of highly nitrogen-doped porous carbon prepared from a metal-organic framework, Nat. Commun. 5 (1) (2014) 5261.
[36] L.-M. Zhang, X.-L. Sui, L. Zhao, G.-S. Huang, D.-M. Gu, Z.-B. Wang, Three-dimensional hybrid aerogels built from graphene and polypyrrole-derived nitrogen-doped carbon nanotubes as a high-efficiency Pt-based catalyst support, Carbon 121 (2017) 518–526.
[37] M.S. Dresselhaus, G. Dresselhaus, R. Saito, A. Jorio, Raman spectroscopy of carbon nanotubes, Phys. Rep. 409 (2) (2005) 47–99.
[38] Z. Li, Z. Xu, X. Tan, H. Wang, C.M.B. Holt, T. Stephenson, B.C. Olsen, D. Mitlin, Mesoporous nitrogen-rich carbons derived from protein for ultra-high capacity battery anodes and supercapacitors, Energy Environ. Sci. 6 (3) (2013) 871–878.
[39] X. Yang, S. Li, H. Huang, J. Li, N. Kobayashi, M. Kubota, Effect of carbon nanoadditives on lithium hydroxide monohydrate-based composite materials for low temperature chemical heat storage, Energies 10 (5) (2017) 644.
[40] Kunimitsu Morishige, Adsorption hysteresis in ordered mesoporous silicas, Adsorption 14 (2-3) (2008) 157–163.
[41] Shijie Li, Hongyu Huang, Jun Li, Noriyuki Kobayashi, Yugo Osaka, Zhaohong He, Haoran Yuan, The effect of 3D carbon nanoadditives on lithium hydroxide monohydrate based composite materials for highly efficient low temperature thermochemical heat storage, RSC Adv. 8 (15) (2018) 8199–8208.
[42] Q. Wang, Y. Xie, B. Ding, G. Yu, F. Ye, C. Xu, Structure and hydration state characterizations of MgSO4-zeolite 13x composite materials for long-term thermochemical heat storage, Sol. Energy Mater. Sol. Cells 200 (2019) 110047.
[43] Y.J. Zhao, R.Z. Wang, Y.N. Zhang, N. Yu, Development of SrBr 2 composite sorbents for a sorption thermal energy storage system to store low-temperature heat, Energy 115 (2016) 129–139.
[44] V. Palomba, A. Sapienza, Y. Aristov, Dynamics and useful heat of the discharge stage of adsorptive cycles for long term thermal storage, Appl. Energy 248 (2019) 299–309.